Homo- and Heterochiral Alkylzinc Fencholates: Linear or Nonlinear Effects in Dialkylzinc Additions to Benzaldehyde

Melanie Steigelmann,[a, b] Yasmin Nisar,[b] Frank Rominger,[b] and Bernd Goldfuss*[a]

Dedicated to Professor Gottfried Huttner on the occasion of his 65th birthday

Abstract: Scalemic mixtures of chiral anisyl fenchols with different *ortho*-substituents (X) in the anisyl moieties [X = H (**1**), Me (**2**), $SiMe_3$ (**3**) and *t*Bu (**4**)] are employed as pre-catalysts in enantioselective additions of diethylzinc to benzaldehyde. While a remarkable asymmetric depletion is apparent for X = H and Me, a linear relationship between the enantiomeric purity of the chiral source and the product 1-phenylpropanol is observed for X = $SiMe_3$ and *t*Bu. X-ray single crystal analyses show that racemic methylzinc fencholates obtained from **1** (X = H) and **2** (X = Me) yield homochiral dimeric complexes, while for **3** (X = $SiMe_3$) and **4** (X = *t*Bu) the heterochiral dimeric alkylzinc structures are formed. The enantiopure fenchols **1**–**4** all yield homochiral dimeric methylzinc complexes. Computed relative energies of homo- and heterochiral fencholate dimers with X = H and Me reveal an intrinsic preference for the formation of the homochiral dimers, consistent with the observed negative NLE. In contrast, similar stabilities are computed for homo- and heterochiral complexes of ligands **3** (X = $SiMe_3$) and **4** (X = *t*Bu), in agreement with the absence of a nonlinear effect for bulky *ortho*-substituents.

Keywords: ab initio calculations · density functional calculations · enantioselectivity · nonlinear effects · X-ray diffraction

Introduction

Enantioselective additions of organozinc reagents to prochiral carbonyl substrates are the subject of intensive research[1] and are frequently applied in syntheses of natural and pharmaceutical products.[2] Current work in this field focuses not only on high enantiomeric excess,[3] but also on mechanistic studies, both with experimental[4] and computational[5] methods. Systematic variation of ligands allows investigations of key steps in these reactions and can reveal the origin of enantioselectivities in combination with computational studies.[6] The achievement of higher enantiomeric purities of the product than of the scalemic[7] catalyst is especially appealing. This nonlinear effect (NLE) was first described quantitatively for asymmetric catalyses by Kagan et al. in 1986.[8] Very strong asymmetric amplifications were found by Noyori et al. employing 3-*exo*-(dimethylamino)isonorborneol (DAIB) as catalyst in the enantioselective addition of diethylzinc to aldehydes.[9] Several more chiral ligands have been found to catalyze additions of organozinc reagents to carbonyl compounds with positive NLE.[10]

[a] Prof. Dr. B. Goldfuss, Dipl.-Chem. M. Steigelmann
Institut für Organische Chemie, Universität zu Köln
Greinstrasse 4, 50939 Köln (Germany)
Fax: (+49) 221-470-5057
E-mail: goldfuss@uni-koeln.de

[b] Dipl.-Chem. M. Steigelmann, Y. Nisar, Dr. F. Rominger
Organisch-Chemisches Institut der Universität Heidelberg
Im Neuenheimer Feld 270, 69121 Heidelberg (Germany)

Asymmetric amplifications (positive NLE) can be explained by the involvement of catalytically inactive, dimeric reservoir species, which are in equilibrium with the active catalyst.[11] Monomeric zinc chelate complexes are known to act as the active species in catalytic additions of diethylzinc to benzaldehyde, while the dimers are unreactive.[12] In a scalemic mixture (*R* and *S*), homochiral dimerization leads to *S*-*S* and *R*-*R* dimers and heterochiral aggregation forms the heterochiral complex *R*-*S* (Scheme 1). If the heterochiral dimer is more thermodynamically stable than the homochiral form, it acts as reservoir species; this in turn results in the enrichment of one monomer (*R* or *S*) and gives rise to asymmetric amplification.[13] If the homochiral complexes are more thermodynamically stable than the heterochiral dimer, an asymmetric depletion (negative NLE) is observed (Scheme 1).[14]

Bidentate anisyl fenchols, prepared by a short stereoselective synthetic route,[6, 15, 16] are known to form dimeric alkylzinc complexes.[17] These ligand systems not only yield complexes with dialkylzinc reagents, but also a variety of chiral aggregates with *n*-butyllithium.[15, 18] Composition of chiral *n*BuLi complexes and enantioselectivities in *n*BuLi additions to benzaldehyde can both be controlled by the *ortho*-substituents in the fencholates. Hence we attempted to synthesize homo- and heterochiral dimers with dimethylzinc and different *ortho*-substituents in the modular anisyl fenchols **1**–**4** (Scheme 2).

Scalemic mixtures of fenchols **1**–**4** (Scheme 2) were employed as pre-catalysts in the enantioselective addition of

  0947-6539/02/0822-5211 $ 20.00+.50/0

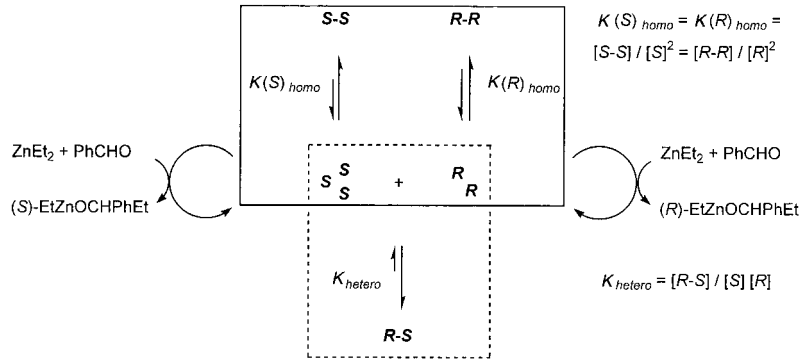

Scheme 1. Origins of positive and negative NLE from hetero- (dashed lines) and homochiral dimerization of monomeric organozinc catalysts.

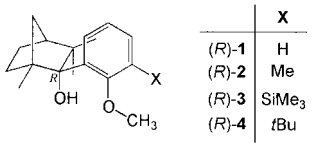

Scheme 2. Modular anisyl fenchols with different *ortho*-substituents X.[19]

diethylzinc to benzaldehyde. The dependence of the product enantioselectivity on the enantiomeric purity of the chiral source was investigated.

Results and Discussion

Different scalemic mixtures of anisyl fenchols **1**–**4** (Scheme 2) were employed as chiral pre-catalysts (5 mol%) in the enantioselective addition of diethylzinc to benzaldehyde (Scheme 3).

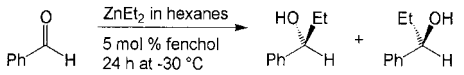

Scheme 3. Enantioselective additions of $ZnEt_2$ to benzaldehyde catalyzed by chiral modular anisyl fenchols **1**–**4** (Scheme 2).

A remarkable negative nonlinear effect was observed for the ligands **1** and **2** with less sterically demanding *ortho*-substituents (X = H and Me) (Figures 1 and 2), while a linear

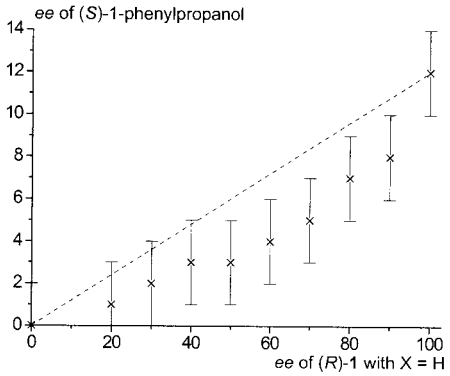

Figure 1. The enantiomeric excess of (*S*)-1-phenylpropanol is shown with its dependence on the enantiomeric purity of the catalyst (*R*)-**1** (X = H). The broken line indicates the linear relation, a remarkable negative deviation from linearity is found.

relationship between the enantiomeric purity of the chiral source and that of the alcoholic product is apparent for the ligands **3** and **4** with the more sterically demanding *ortho*-substituents $SiMe_3$ and *t*Bu (Figures 3 and 4).

Due to the central role of dimeric *R-R*, *S-S* and *R-S* complexes in the catalytic cycle (Scheme 1), the propensity of formation of these methylzinc anisyl fencholate dimers is of principal interest. An equimolar mixture of racemic fenchol **1** and dimethylzinc in toluene yields a colorless solid, which can be analyzed by X-ray crystal diffraction after recrystallization.[20] Surprisingly, the homochiral dimeric methylzinc chelate complexes $(R\text{-}\mathbf{1})_2$ and $(S\text{-}\mathbf{1})_2$ are formed (Scheme 4), but no heterochiral dimer was found.[21]

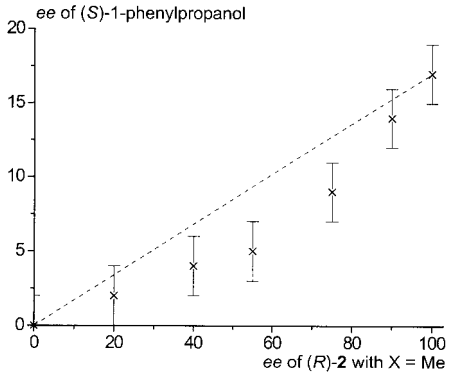

Figure 2. The enantiomeric excess of (*S*)-1-phenylpropanol is shown with its dependence on the enantiomeric purity of the catalyst (*R*)-**2** (X = Me). The broken line indicates the linear relation, a remarkable negative deviation from linearity is found.

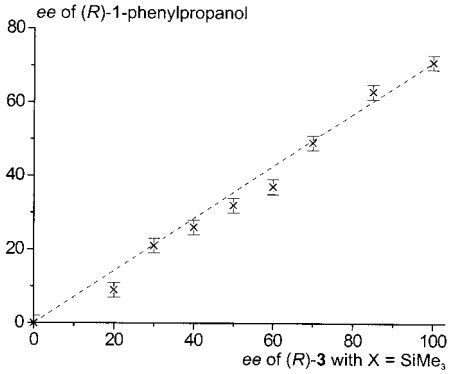

Figure 3. The enantiomeric excess of (*R*)-1-phenylpropanol is shown with its dependence on the enantiomeric purity of the catalyst (*R*)-**3** (X = $SiMe_3$). The broken line indicates the linear relation that is observed.

The enantiopure ligand (*R*)-**1** and dimethylzinc also form the homochiral complex $(R\text{-}\mathbf{1})_2$ (X-ray crystal structure in Figure 5).[17b] The dimeric C_2-symmetrical methylzinc chelate complex $(R\text{-}\mathbf{1})_2$ contains a four-membered Zn_2O_2 ring in the

0947-6539/02/0822-5212 $ 20.00+.50/0 *Chem. Eur. J.* **2002**, *8*, No. 22

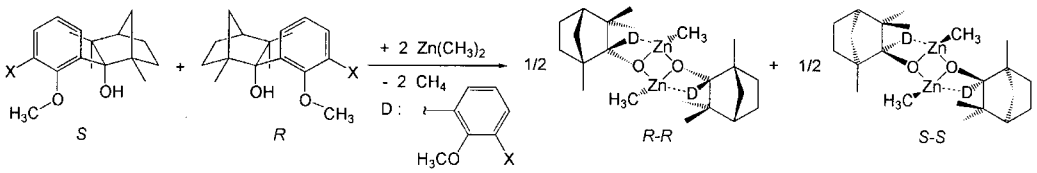

Scheme 4. Homochiral dimers formed from equimolar mixtures of racemic ligand **1** (X = H) or **2** (X = Me) and dimethylzinc in toluene (X-ray crystal structures of $(R\text{-}\mathbf{1})_2$ in Figure 5 and of $(R\text{-}\mathbf{2})_2$ in Figure 6).[21]

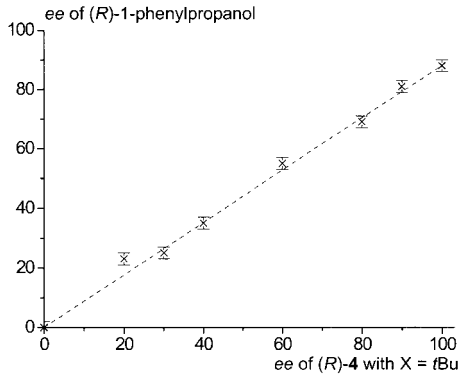

Figure 4. The enantiomeric excess of (*R*)-1-phenylpropanol is shown with its dependence on the enantiomeric purity of the catalyst (*R*)-**4** (X = *t*Bu). The broken line indicates the linear relation that is observed.

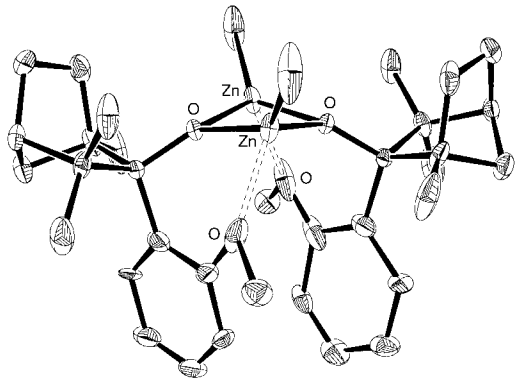

Figure 5. X-ray crystal structure of $(R\text{-}\mathbf{1})_2$[16b] (X = H) crystallized from an enantiopure mixture of (*R*)-**1** and dimethylzinc: the methyl groups on the zinc atoms and the methoxy groups are aligned *syn* to the Zn_2O_2 plane (C_2 symmetry). Selected bond lengths and angles are given in Table 2.

center. The two methyl groups on the zinc ions are aligned *syn* with respect to this Zn_2O_2 plane. The methoxy groups in the aryl moieties of the ligands also coordinate *syn* to the zinc centers, but from opposite sides with respect to the methyl units (Figure 5).

As for fenchol **1** (X = H), crystals of the homochiral dimers $(R\text{-}\mathbf{2})_2$ and $(S\text{-}\mathbf{2})_2$ are obtained from an equimolar mixture of racemic ligand **2** (X = Me) and dimethylzinc in toluene (Scheme 4).[19] The homochiral complex $(R\text{-}\mathbf{2})_2$ is also formed by the enantiopure ligand (*R*)-**2** and dimethylzinc (see the X-ray crystal structure in Figure 6). The position of the methyl units on the zinc ions and the methoxy groups of the ligand fragments is *syn* with respect to the Zn_2O_2 ring (Figure 6), similar to $(R\text{-}\mathbf{1})_2$ (Figure 5).

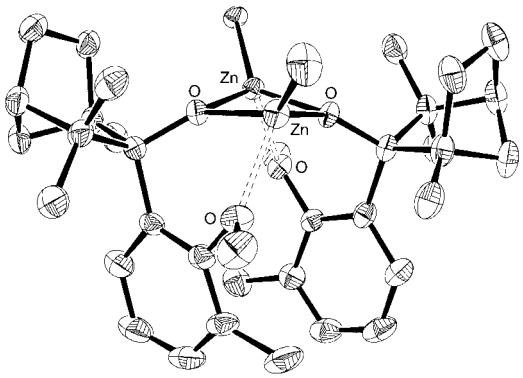

Figure 6. X-ray crystal structure of $(R\text{-}\mathbf{2})_2$ (X = Me) crystallized from an enantiopure mixture of (*R*)-**2** and dimethylzinc: the methyl groups on the zinc atoms and the methoxy groups are aligned *syn* to the Zn_2O_2 plane. Selected bond lengths and angles are given in Table 2.

In contrast to the results for ligands **1** and **2** (Scheme 4), an equimolar mixture of racemic fenchol **3** and dimethylzinc in toluene yields the heterochiral dimeric complex (*R*-**3**)(*S*-**3**) (Scheme 5, X-ray crystal structure in Figure 7).

The X-ray crystal analysis of the obtained dimeric chelate complex (*R*-**3**)(*S*-**3**) discloses an *anti*-alignment of the methylzinc moieties and the two coordinating methoxy groups of the ligand molecules with regard to the Zn_2O_2 ring (C_i symmetry, Figure 7). Like **3**, a racemic mixture of ligand **4** forms with dimethylzinc in a 1:1 ratio forms the dimeric complex (*R*-**4**)(*S*-**4**) (Scheme 5, X-ray crystal structure of which is shown in Figure 8). In the dimeric C_i-symmetric methylzinc chelate complex (*R*-**4**)(*S*-**4**) the two methyl groups on the zinc atoms and the methoxy groups in the aryl moieties of the ligands are aligned *anti* with respect to the Zn_2O_2 plane (Figure 8).

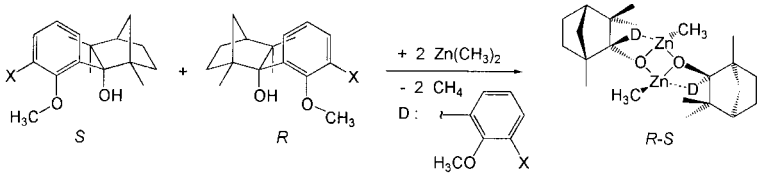

Scheme 5. Heterochiral dimers formed from equimolar mixtures of racemic ligand **3** (X = $SiMe_3$) or **4** (X = *t*Bu) and dimethylzinc in toluene (X-ray crystal structures of (*R*-**3**)(*S*-**3**) in Figure 7 and of (*R*-**4**)(*S*-**4**) in Figure 8).

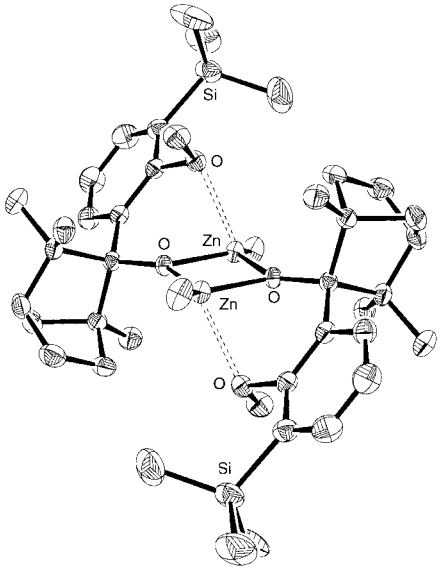

Figure 7. X-ray crystal structure of (*R*-**3**)(*S*-**3**) (X = $SiMe_3$): the methyl groups on the zinc atoms and the methoxy groups are aligned *anti* to the Zn_2O_2 plane (C_i symmetry). Selected bond lengths and angles are given in Table 2.

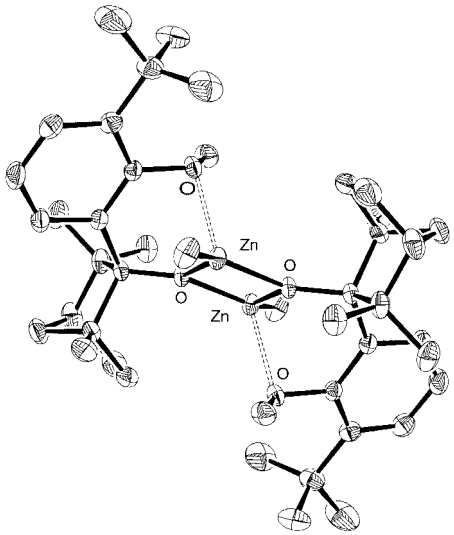

Figure 8. X-ray crystal structure of (*R*-**4**)(*S*-**4**) (X = *t*Bu): the methyl groups on the zinc atoms and the methoxy groups are aligned *anti* to the Zn_2O_2 plane (C_i symmetry). Selected bond lengths and angles are given in Table 2.

To characterize the homochiral dimers of ligands **3** and **4**, one equivalent of the enantiopure ligand was treated with one equivalent of dimethylzinc to give (*R*-**3**)$_2$,[6b] and (*R*-**4**)$_2$, respectively (Scheme 6).

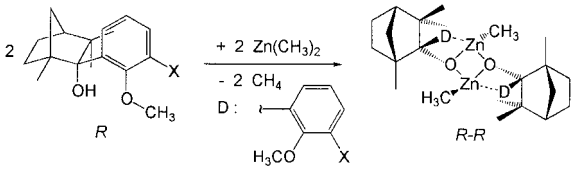

Scheme 6. Homochiral dimers formed from equimolar mixtures of enantiopure ligand **3** (X = $SiMe_3$)[6b] or **4** (X = *t*Bu) and dimethylzinc in toluene (X-ray crystal structures of (*R*-**3**)$_2$ in Figure 9 and of (*R*-**4**)$_2$ in Figure 10).

The structural arrangements in the dimeric complexes (*R*-**3**)$_2$ (Figure 9) and (*R*-**4**)$_2$ (Figure 10) are different compared to (*R*-**1**)$_2$ (Figure 5) and (*R*-**2**)$_2$ (Figure 6): the more sterically demanding substituents $SiMe_3$ and *t*Bu change the symmetry

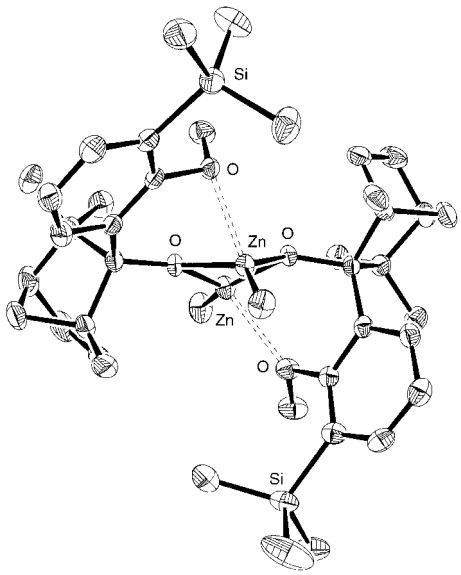

Figure 9. X-ray crystal structure of (*R*-**3**)$_2$[6b](X = $SiMe_3$): the methyl groups on the zinc atoms are aligned *syn* to the Zn_2O_2 plane and the methoxy groups coordinate *anti* to the zinc centers. Selected bond lengths and angles are given in Table 2.

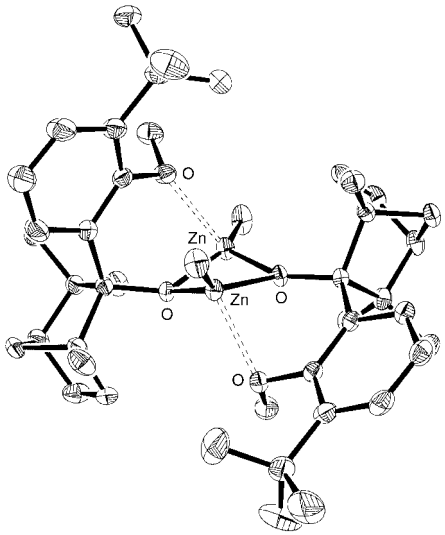

Figure 10. X-ray crystal structure of (*R*-**4**)$_2$ (X = *t*Bu): the methyl groups on the zinc atoms are aligned *syn* to the Zn_2O_2 plane and the methoxy groups coordinate *anti* to the zinc centers. Selected bond lengths and angles are given in Table 2.

relative to X = H and Me. In contrast to the homochiral complexes (*R*-**1**)$_2$ (X = H) and (*R*-**2**)$_2$ (X = Me), the methoxy groups of the two ligands in (*R*-**3**)$_2$ (X = $SiMe_3$) and (*R*-**4**)$_2$ (X = *t*Bu) are now in *trans*-positions on the central four membered Zn_2O_2 ring.

Because the heterochiral dimeric fencholate zinc complexes with the *ortho*-substituents X = H or Me were not accessible experimentally, ab initio (RHF/LanL2DZ (Zn, Si)/

0947-6539/02/0822-5214 $ 20.00+.50/0 *Chem. Eur. J.* **2002**, *8*, No. 22

3-21G (C, H, O)[22] computations were employed using GAUSSIAN 98[23] to reveal the relative energies of both homo- and heterochiral structures (energies for optimized dimers with X = H and Me are shown in Table 1). If the methyl groups on the zinc atoms and the methoxy groups of the ligand fragments in $(R\text{-}\mathbf{1})_2$ (Figure 5) are arranged *syn*, the complex is favored by 5.2 kcal mol^{-1} compared with the *anti* case (Table 1). This *syn*-homodimer is also 4.1 kcal mol^{-1} more stable than the calculated *syn*-heterodimer (Table 1). For X = Me, the *syn*-homodimer $(R\text{-}\mathbf{2})_2$ (Figure 6) is 1.1 kcal mol^{-1} more stable than the *anti*-structure and preferred by 3.8 kcal mol^{-1} compared to the C_i-symmetric *anti*-heterodimer (Table 1). The theoretically determined energies reveal that, in these two cases (X = H and Me), the experimentally obtained *syn*-homodimers are the intrinsically most stable structures.

Table 1. Computed relative energies [au] for the structures of dimeric zinc chelate complexes.

	E [au][a]		E [au][a]		E [au][b]
$(R\text{-}\mathbf{1})_2$ (*syn*)	– 1810.7732	$(R\text{-}\mathbf{2})_2$ (*syn*)	– 1888.4034	$(R\text{-}\mathbf{3})(S\text{-}\mathbf{3})$[c]	– 2080.5603
$(R\text{-}\mathbf{1})_2$ (*anti*)	– 1810.7650	$(R\text{-}\mathbf{2})_2$ (*anti*)	– 1888.4016	$(R\text{-}\mathbf{3})_2$[d]	– 2080.5555
$(R\text{-}\mathbf{1})(S\text{-}\mathbf{1})$ (*syn*)	– 1810.7667	$(R\text{-}\mathbf{2})(S\text{-}\mathbf{2})$ (*syn*)	– 1888.3851	$(R\text{-}\mathbf{4})(S\text{-}\mathbf{4})$[e]	– 2148.9502
$(R\text{-}\mathbf{1})(S\text{-}\mathbf{1})$ (*anti*)	– 1810.7603	$(R\text{-}\mathbf{2})(S\text{-}\mathbf{2})$ (*anti*)	– 1888.3974	$(R\text{-}\mathbf{4})_2$[f]	– 2148.9487

[a] Optimized methylzinc fencholate dimers (RHF/LanL2DZ (Zn)/3-21G (C, H, O)). [b] Single-point computations (X-ray geometries: B3LYP/LanL2DZ (Zn, Si)/6-31G* (C, H, O)). [c] See Figure 7. [d] See Figure 9. [e] See Figure 8. [f] See Figure 10.

The observed negative nonlinear effect for X = H and Me as *ortho*-substituents can be explained by thermodynamically more stable homochiral dimers. The equilibrium for the enantiomer, which is present in excess, will be shifted more to the side of its homochiral dimer. Consequently, this enantiomer is partly captured as the unreactive dimer and so the excess of its monomer in solution is smaller than expected. The diminished excess of the monomer, which controls the stereochemistry of the reaction, then leads to the observed negative NLE.

To explain the observed linear effect for X = $SiMe_3$ and *t*Bu as *ortho*-substituents, the homo- and heterochiral dimeric complexes should exhibit comparable stabilities. The formation of both homo- and heterochiral dimers was observed for the ligands **3** (X = $SiMe_3$) and **4** (X = *t*Bu), while **1** (X = H) and **2** (X = Me) formed only homochiral dimers. X-ray crystal analyses of the dimeric structures reveal similar lengths of the external Zn–O bond, which is the dimer forming bond, as a feature of stability of the dimers, in $(R\text{-}\mathbf{3})_2$ and $(R\text{-}\mathbf{3})(S\text{-}\mathbf{3})$ (2.03 Å, 1.98 Å: difference 0.05 Å; Table 2) and also in $(R\text{-}\mathbf{4})_2$ and $(R\text{-}\mathbf{4})(S\text{-}\mathbf{4})$ (2.01 Å, 1.97 Å: difference 0.04 Å; Table 2). Hence, the homo- and heterochiral dimers should have an equal propensity to dissociate into their catalytically active monomers.

To verify that the homo- and heterochiral dimeric complexes possess similar stabilities, single point energies were computed with geometries obtained from X-ray crystal structures for $(R\text{-}\mathbf{3})_2$ versus $(R\text{-}\mathbf{3})(S\text{-}\mathbf{3})$ and for $(R\text{-}\mathbf{4})_2$ versus $(R\text{-}\mathbf{4})(S\text{-}\mathbf{4})_2$. The heterochiral dimeric organozinc chelate complex of the ligand system with X = $SiMe_3$ $(R\text{-}\mathbf{3})(S\text{-}\mathbf{3})$ was found to be 3.0 kcal mol^{-1} more stable than the homochiral dimer $(R\text{-}\mathbf{3})_2$ (Table 1). In case of *t*Bu, the computed higher stability of $(R\text{-}\mathbf{4})_2$ relative to $(R\text{-}\mathbf{4})(S\text{-}\mathbf{4})$ is 0.9 kcal mol^{-1} (Table 1). The computed energies confirm the assumption that the stabilities of the hetero- and homochiral dimers for ligands **3** and **4** with the sterically demanding *ortho*-substituents X = *t*Bu and $SiMe_3$ are very similar (Scheme 2).

The *ortho*-substituents X force a distortion of the ligand systems in all dimeric complexes, depending on their steric demands. The methyl substituent in $(R\text{-}\mathbf{2})_2$ produces a slight distortion of the ligand system compared to the unsubstituted complex $(R\text{-}\mathbf{1})_2$: in $(R\text{-}\mathbf{2})_2$ the methoxy group is bending out of the aryl plane (C7-O6-C5-C8 = – 57.3° for X = Me; – 28.8° for X = H; Scheme 7, Table 2).

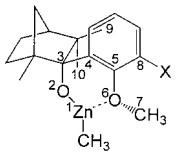

Scheme 7. Numbering of selected atoms in the chelating methyl zinc fencholates. For bond lengths and angles see Table 2.

As a consequence, the repulsive interaction increases due to close contact between the methoxy and the *exo*-methyl group (C9) of the bicycloheptane moiety (C7 ··· C9 3.63 Å for X = Me; 3.86 Å for X = H; Scheme 7, Table 2). This results from rotation around the C3–C4 axis in a more coplanar arrangement of the O2-C3-C4-C5 unit (45.7° in $(R\text{-}\mathbf{2})_2$; 50.8° in $(R\text{-}\mathbf{1})_2$, Table 2) and finally in a shorter O6–Zn1 distance of 2.16 Å for $(R\text{-}\mathbf{2})_2$ (X = Me) compared to 2.21 Å for $(R\text{-}\mathbf{1})_2$ (X = H) without *ortho*-substitution. The described effect does not change the basic C_2-symmetric geometry of complex $(R\text{-}\mathbf{2})_2$, but even more

Table 2. Selected bond distances [Å] and angles [°] in the X-ray crystal structures of dimeric zinc chelate complexes.

	C7-O6-C5-C8	C7 ··· C9/10	O2-C3-C4-C5	O6 ··· Zn1	Zn–$O_{internal}$[a]	Zn–$O_{external}$[b]
$(R\text{-}\mathbf{1})_2$[c]	– 28.8	3.86	50.8	2.21	1.97	2.01
$(R\text{-}\mathbf{2})_2$[d]	– 57.3/ – 57.3	3.61/3.63	46.3/45.7	2.17/2.15	1.98/1.97	2.01/2.02
$(R\text{-}\mathbf{3})_2$[e]	– 55.6/ – 101.4	3.55/3.56	48.3/29.0	2.40/2.27	1.95/1.98	2.02/2.04
$(R\text{-}\mathbf{4})_2$[f]	– 65.5/ – 106.1	3.62/3.45	37.4/27.5	2.37/2.27	1.97/1.98	2.01
$(R\text{-}\mathbf{3})(S\text{-}\mathbf{3})$[g]	– 105.0	3.52	28.6	2.37	1.99	1.98
$(R\text{-}\mathbf{4})(S\text{-}\mathbf{4})$[h]	– 111.5	3.41	29.4	2.38	1.99	1.97

[a] O2–Zn1 (Scheme 7). [b] Dimer forming bond connecting the zinc fencholate moieties. [c] X = H, Figure 5,[17] crystallographic C_2 symmetry. [d] X = Me, Figure 6. [e] X = $SiMe_3$, Figure 9[6b]. [f] X = *t*Bu, Figure 10. [g] X = $SiMe_3$, Figure 7, crystallographic C_i symmetry. [h] X = *t*Bu, Figure 8, crystallographic C_i symmetry.

  0947-6539/02/0822-5215 $ 20.00+.50/0

sterically demanding substituents such as $SiMe_3$ and *t*Bu will lead to a different structure. In the dimeric complexes $(R\text{-}\mathbf{3})_2$ and $(R\text{-}\mathbf{4})_2$ the methoxy groups coordinate *anti* to the zinc centers. The distortion found in $(R\text{-}\mathbf{2})_2$ compared with $(R\text{-}\mathbf{1})_2$ continues for X = $SiMe_3$ and *t*Bu in the homochiral structures $(R\text{-}\mathbf{3}/\mathbf{4})_2$ as well as in the heterochiral complexes (*R*-**3**/**4**)-(*S*-**3**/**4**) (Table 2). The methoxy group is bending out of the aryl plane and subsequently a repulsive interaction arises from closer contacts between this methoxy and the geminal dimethyl unit of the bicycloheptane moiety.[24] This results from rotation about the C3–C4 axis in a more coplanar arrangement of the O2-C3-C4-C5 unit.

Similar distortions are also apparent in computationally-optimized structures for the dimeric methylzinc fencholates in the *syn*-homo forms $(R\text{-}\mathbf{1})_2$ and $(R\text{-}\mathbf{2})_2$ (Table 3).

Table 3. Selected bond distances [Å] and angles [°] in the geometry optimized structures[a] of the *syn*-homodimers $(R\text{-}\mathbf{1})_2$ and $(R\text{-}\mathbf{2})_2$.

	C7-O6-C5-C8	C7···C10	O2-C3-C4-C5	O6···Zn1	Zn–$O_{internal}$[b]	Zn–$O_{external}$[c]
$(R\text{-}\mathbf{1})_2$	−40.4	3.60	45.1	2.11	2.00	2.02
$(R\text{-}\mathbf{2})_2$	−60.4/−59.8	3.56/3.58	42.8/41.4	2.11/2.12	1.99/2.00	2.02/2.03

[a] RHF/LanL2DZ (Zn)/3-21G (C, H, O). [b] Zn1–O7, (Scheme 7). [c] Dimer-forming bond connecting the zinc fencholate moieties.

The chemical yields in the enantioselective diethylzinc additions to benzaldehyde catalyzed by the ligands **1**–**4** increase in this order: X = *t*Bu, 47%; X = H, 59%; X = Me, 73%; X = $SiMe_3$, 85%). Higher yields correspond to higher reactivity. The observed inversion of the stereoselectivity in the product alcohol for the ligand systems with X = $SiMe_3$ and *t*Bu (Figures 3 and 4) compared to X = H and Me (Figures 1 and 2) can be explained by comparison of computed μ-O transition structures and has been reported recently.[6a]

Conclusion

A remarkable negative NLE is apparent for the anisyl fenchols with X = H (**1**) and Me (**2**) employed as pre-catalysts in enantioselective additions of diethylzinc to benzaldehyde, while a linear dependence of enantioselectivities is found for X = $SiMe_3$ (**3**) and *t*Bu (**4**) (Scheme 2). With dimethylzinc, ligands **1** and **2** exclusively form homochiral dimeric complexes, even from racemic mixtures of the ligands (see X-ray analyses in Figures 5 and 6). The experimentally formed *syn*-homodimers (for X = H and Me) are also computed to be preferred over heterochiral structures. An explanation for the appearance of the asymmetric depletion (negative NLE) for **1** and **2** originates from equilibria of monomeric and homodimeric alkylzinc fencholates (Scheme 1): the excess of one enantiomer of the monomeric alkylzinc fencholate is lowered by a stronger shifting of its monomer–dimer equilibrium in favor of the catalytically inactive homochiral dimer. A linear relationship for anisyl fenchols in diethylzinc additions to benzaldehyde was observed with the more sterically demanding *ortho*-substituents in **3** (X = $SiMe_3$) and in **4** (X = *t*Bu). These fenchols give rise to the formation of heterochiral dimeric methylzinc fencholate complexes with racemic ligands and homochiral dimeric complexes with enantiopure ligands. The computed single point energies of the experimental structures show small energy differences between homo- and heterochiral dimeric structures ($(R\text{-}\mathbf{3})_2$ vs (*R*-**3**)-(*S*-**3**) and $(R\text{-}\mathbf{4})_2$ vs (*R*-**4**)(*S*-**4**), Figures 7–10), consistent with similar stabilities of homo- and heterochiral dimers and equal propensities for dissociation into catalytically-active monomers. These results demonstrate that the nature of the *ortho*-substituents in the anisyl moieties of the fenchol ligands control the stability of homo- and heterochiral dimers. Hence, a close correspondence between the structural changes in the ligand systems and the appearance of nonlinear effects in enantioselective diethylzinc additions is demonstrated for modular anisyl fencholates.

Experimental Section

General methods: Reactions were carried out under an argon atmosphere (Schlenk and needle/septum techniques) with dried and degassed solvents. X-ray crystal analyses were performed on a Bruker Smart CCD diffractometer with $Mo_{K\alpha}$ radiation at 200 K. Data sets corresponding to a complete sphere of data were collected using 0.3° ω scans. The structures were solved using direct methods, least-squares refinement, and Fourier techniques. Hydrogen atoms were taken into account at geometrically calculated positions. NMR Spectra were recorded on a Bruker AC300 and DRX500 spectrometer. GC analyses were carried out with a Chrompack machine [WCOT Fused Silica CP-SIL-5CB, 10 m length, 0.32 mm diameter] and HPLC analyses on a HP-1100 machine [Chiracel OD-H column, hexanes/*i*PrOH 99.2:0.8, 1 mL min^{-1}, 26 °C, 254 nm, 1-phenylpropanol: t_R = 16.5 min (*R*), 20.3 min (*S*)]. CCDC-185287 ($(R\text{-}\mathbf{1})_2$), CCDC-185288 ($(R\text{-}\mathbf{2})_2$), CCDC-185289 ($(R\text{-}\mathbf{2})_2$), CCDC-185290 ((*R*-**3**)(*S*-**3**)), CCDC-185291 ((*R*-**4**)(*S*-**4**)), CCDC-185292 ($(R\text{-}\mathbf{4})_2$) contain the supplementary crystallographic data for this paper. These data can be obtained free of charge via www.ccdc.cam.ac.uk/conts/retrieving.html (or from the Cambridge Crystallographic Data Centre, 12 Union Road, Cambridge CB2 1EZ, UK; (fax: (+44) 1223-336-033; or e-mail: deposit@ccdc.cam.ac.uk).

General synthesis of homochiral dimeric complexes with ligand systems (*R*)-2 and (*R*)-4: A solution of dimethylzinc (0.2 mmol, 2 M, 0.1 mL) in toluene was added to the ligand (0.2 mmol of (*R*)-ligand) at RT. After cooling the solution to −80 °C and thawing three times, the precipitate formed was dissolved in hot toluene. Slow cooling to room temperature yielded the homochiral dimer as colorless crystals.

Characterization of $(R\text{-}\mathbf{2})_2$: Yield: 39%; m.p. >190 °C, glassy, 213 °C; elemental analysis calcd (%): C 66.44, H 8.03; found: C 66.45, H 8.03; ^{1}H NMR (300 MHz, [D_8]toluene, −10 °C): δ = −0.10 (s, 3H; $ZnCH_3$), 0.50 (s, 3H; CH_3), 1.27 (m, 1H; CH_2), 1.30 (m, 1H; CH_2), 1.36 (m, 1H; CH_2/s, 3H; CH_3), 1.45 (s, 3H; CH_3), 1.51 (m, 1H; CH_2), 1.58 (s, 3H; CH_3), 1.66 (s, 1H; CH), 1.93 (m, 1H; CH_2), 2.37 (m, 1H; CH_2), 3.34 (s, 3H; OCH_3), 6.46 (d, ^3J = 7.35 Hz, 1H; H_{Ar}), 6.62 (t, ^3J = 7.73 Hz, 1H; H_{Ar}), 7.28 (d, ^3J = 7.89 Hz, 1H; H_{Ar}); ^{13}C NMR (75 MHz, [D_8]toluene, −10 °C) δ = −7.5 ($ZnCH_3$), 17.4 (CH_3), 18.5 (CH_3), 22.1 (CH_3), 25.1 (CH_2), 25.9 (CH_3), 34.6 (CH_2), 42.4 (CH_2), 45.9 (C_q), 51.2 (CH), 55.0 (C_q), 63.5 (OCH_3), 90.1 (C_q), 122.4 (C_{Ar}), 126.5 (C_{Ar}), 130.6 (C_{Ar}), 136.5 ($C_{q,Ar}$), 141.0 ($C_{q,Ar}$), 157.6 ($C_{q,Ar}$). X-ray crystal data of $(R\text{-}\mathbf{2})_2$: $C_{45}H_{64}O_4Zn_2$ (with crystal toluene), M = 799.70, space group $P2_12_12_1$, a = 11.2793(2), b = 17.5088(2), c = 20.6155(2) Å; V = 4071.29(9) Å^3, Z = 4, T = 200(2) K, μ = 1.219 mm^{-1}, reflections total: 42573, unique: 9334, observed: 8198 ($I > 2\sigma(I)$), parameters refined: 473, $R1$ = 0.029, $wR2$ = 0.068, GOF_{all} = 1.01.

Characterization of $(R\text{-}\mathbf{4})_2$: Yield: 27%; m.p. 201 °C (decomp); elemental analysis calcd (%): C 66.75, H 8.65; found: C 66.71, H 8.49; ^{1}H NMR

0947-6539/02/0822-5216 $ 20.00+.50/0 *Chem. Eur. J.* **2002**, *8*, No. 22

(500 MHz, [D$_8$]toluene, −10 °C): $\delta = -0.76$ (s, 3H; $ZnCH_3$), −0.10 (s, 3H; $ZnCH_3$), 0.73 (s, 6H; $2CH_3$), 1.23 (m, 4H; 2CH*H*, 2C*H*H), 1.30 (s, 12H; 4CH_3), 1.40 (s, 18H; 2*t*Bu), 1.49 (m, 4H; 2CH*H*, 2C*H*H), 1.71 (s, 2H; CH), 2.52 (m, 2H; 2CH*H*), 2.73 (m, 2H; 2C*H*H), 3.79 (s, 6H; 2OCH_3), 6.81 (m, 2H; H_{Ar}), 7.13 (d, $^3J = 6.70$ Hz, 2H; H_{Ar}), 7.56 (d, $^3J = 7.35$ Hz, 2H; H_{Ar}); ^{13}C NMR (75 MHz, [D$_8$]toluene, 25 °C) $\delta = -6.0$ ($ZnCH_3$), 18.5 (CH_3), 22.4 (CH_3), 24.4 (CH_2), 31.8 (CH_3), 32.9 (C(CH_3)$_3$), 35.8 (*C*(CH_3)$_3$), 36.2 (CH_2), 42.3 (CH_2), 43.6 (C_q), 50.1 (CH), 55.1 (C_q), 65.9 (OCH_3), 87.0 (C_q), 122.4 (C_{Ar}), 127.0 (C_{Ar}), 130.2 (C_{Ar}), 140.8 (C_{Ar}), 143.4 (C_{Ar}), 158.7 (C_{Ar}). X-ray crystal data of (*R*-**4**)$_2$: $C_{44}H_{68}O_4Zn_2$, $M = 791.72$, space group $P2_1$, $a = 13.3952(1)$, $b = 10.6271(1)$, $c = 14.1778(1)$ Å; $\beta = 92.355(1)°$, $V = 2016.54(3)$ Å^3, $Z = 2$, $T = 200(2)$ K, $\mu = 1.230\,mm^{-1}$, reflections total: 20948, unique: 9000, observed: 8455 ($I > 2\sigma(I)$), parameters refined: 467, $R1 = 0.028$, $wR2 = 0.069$, $GOF_{all} = 1.02$.

Synthesis and characterization of (*R*-1)$_2$: A solution of dimethylzinc (0.2 mmol, 2 M, 0.1 mL) in toluene was added to a racemic mixture of **1** (0.1 mmol of (*R*)- and 0.1 mmol of (*S*)-ligand). The solution was stirred for 20 minutes and then held at room temperature over night. Colorless crystals of (*R*-**1**)$_2$ were obtained (35%). M.p. 170 °C (decomp); elemental analysis calcd (%): C 63.63, H 7.71; found: C 62.32, H 7.72; ^{1}H NMR (500 MHz, [D$_8$]toluene, +10 °C): $\delta = -0.14$ (s, 3H; $ZnCH_3$), 0. 55 (s, 3H; CH_3), 1.23 (m, 1H; CH_2), 1.30 (s, 3H; CH_3), 1.48 (m, 2H; $2CH_2$), 1.52 (s, 3H; CH_3), 1.74 (m, 2H; CH, CH_2), 1.93 (m, 1H; CH_2), 2.25 (m, 1H; CH_2), 2.97 (s, 3H; OCH_3), 6.33 (d, $^3J = 7.82$ Hz, 1H; H_{Ar}), 6.79 (td, $^3J = 7.58$ Hz, $^4J = 0.98$ Hz, 1H; H_{Ar}), 6.94 (td, $^3J = 7.58$ Hz, $^4J = 1.47$ Hz, 1H; H_{Ar}), 7.53 (dd, $^3J = 7.82$ Hz, $^4J = 0.98$ Hz, 1H; H_{Ar}); ^{13}C NMR (125 MHz, [D$_8$]toluene, +10 °C) $\delta = -8.0$ ($ZnCH_3$), 18.3 (CH_3), 22.6 (CH_3), 25.3 (CH_2), 29.4 (CH_3), 33.4 (CH_2), 41.9 (CH_2), 44.5 (C_q), 50.8 (CH), 53.4 (C_q), 54.0 (OCH_3), 88.7 (C_q), 110.8 (C_{Ar}), 119.6 (C_{Ar}), 126.9 (C_{Ar}), 132.8 ($C_{q,Ar}$), 137.3 (C_{Ar}), 157.4 ($C_{q,Ar}$); X-ray crystal data of (*R*-**1**)$_2$: $C_{36}H_{52}O_4Zn_2$, $M = 679.52$, space group $P2_1/c$, $a = 19.3720(1)$, $b = 10.3617(1)$, $c = 18.0310(1)$ Å; $\beta = 112.668(1)°$, $V = 3339.73(4)$ Å^3, $Z = 4$, $T = 200(2)$ K, $\mu = 1.473\,mm^{-1}$, reflections total: 37869, unique: 8982, observed: 7564 ($I > 2\sigma(I)$), parameters refined: 389; $R1 = 0.025$, $wR2 = 0.063$, $GOF_{all} = 1.02$.

Synthesis and characterization of (*R*-2)$_2$: A solution of dimethylzinc (0.2 mmol, 2 M, 0.1 mL) in toluene was added to a racemic mixture of the ligand (0.1 mmol of (*R*)- and 0.1 mmol of (*S*)-ligand) at RT. After freezing the solution to −80 °C and thawing three times, the precipitate formed was dissolved in hot toluene. Slow cooling to room temperature yielded the homochiral dimer as colorless crystals (40%). M.p. 223–230 °C (decomp); elemental analysis calcd (%): C 64.50, H 7.98; found: C 64.13, H 7.89; ^{1}H NMR (500 MHz, [D$_8$]toluene, +10 °C): $\delta = -0.18$ (s, 3H; $ZnCH_3$), 0. 45 (s, 3H; CH_3), 1.20 (m, 1H; CH_2), 1.24 (m, 1H; CH_2), 1.30 (s, 3H; CH_3), 1.44 (s, 3H; $C_{Ar}CH_3$), 1.47 (m, 1H; CH_2), 1.54 (s, 3H; CH_3), 1.60 (s, 1H; CH), 1.87 (m, 1H; CH_2), 2.32 (m, 1H; CH_2), 3.16 (m, 1H; CH_2), 3.35 (s, 3H, OCH_3), 6.44 (d, $^3J = 7.13$ Hz, 1H; H_{Ar}), 6.59 (t, $^3J = 7.69$ Hz, 1H; H_{Ar}), 7.26 (d, $^3J = 7.68$ Hz, 1H; H_{Ar}); ^{13}C NMR (125 MHz, [D$_8$]toluene, +10 °C) $\delta = -7.5$ ($ZnCH_3$), 17.3 (CH_3), 18.5 (CH_3), 22.0 (CH_3), 25.3 (CH_2), 25.8 (CH_3), 34.4 (CH_2), 42.3 (CH_2), 45.1 (C_q), 51.1 (CH), 54.9 (C_q), 63.5 (OCH_3), 89.8 (C_q), 121.9 (C_{Ar}), 126.5 (C_{Ar}), 130.1 (C_{Ar}), 136.4 ($C_{q,Ar}$), 140.9 ($C_{q,Ar}$), 157.5 ($C_{q,Ar}$); X-ray crystal data of (*R*-**2**)$_2$: $C_{38}H_{56}O_4Zn_2$, $M = 707.57$, space group $P2_1/c$, $a = 20.0453(2)$, $b = 10.4315(2)$, $c = 18.0755(1)$ Å; $\beta = 113.621(1)°$, $V = 3462.96(8)$ Å^3, $Z = 4$, $T = 200(2)$ K, $\mu = 1.423\,mm^{-1}$, reflections total: 35002, unique: 7938, observed: 6527 ($I > 2\sigma(I)$), parameters refined: 409, $R1 = 0.026$, $wR2 = 0.064$, $GOF_{all} = 1.05$.

General synthesis of heterochiral dimeric complexes with ligands 3 and 4: A solution of dimethylzinc (0.2 mmol, 2 M, 0.1 mL) in toluene was added to a racemic mixture of the ligand (0.1 mmol of (*R*)- and 0.1 mmol of (*S*)-ligand) at RT. After freezing the solution to −80 °C and thawing three times, the precipitate formed was dissolved in hot toluene. Slow cooling to room temperature yielded the heterochiral dimer as colorless crystals.

Characterization of (*R*-3)(*S*-3): Yield: 74%; m.p. 230 °C; elemental analysis calcd (%): C 61.23, H 8.32; found: C 61.34, H 8.46; ^{1}H NMR (500 MHz, [D$_8$]toluene, −10 °C): $\delta = -1.27$ (s, 3H; $ZnCH_3$), −0.90 (s, 6H; 2$ZnCH_3$), −0.11 (s, 3H; $ZnCH_3$), 0.35 (s, 18H; 2Si(CH_3)$_3$), 0.38 (s, 18H; 2Si(CH_3)$_3$), 0. 59 (s, 6H; 2CH_3), 0.67 (s, 6H; 2CH_3), 1.21 (m, 4H;, 2C*H*H, 2CH*H*), 1.25 (m, 4H; 2C*H*H, 2CH*H*), 1.28 (s, 6H; 2CH_3), 1.31 (s, 6H; 2CH_3), 1.37 (s, 6H; 2CH_3), 1.40 (s, 6H; 2CH_3), 1.51 (m, 4H; 2C*H*H, 2CH*H*), 1.63 (s, 2H; 2CH), 1.67 (s, 2H; 2CH), 1.88 (m, 2H; 2C*H*H), 2.00 (m, 2H; 2CH*H*), 2.44 (m, 4H; 2 C*H*H, 2CH*H*), 2.54 (m, 2H; 2C*H*H), 2.61 (m, 2H; 2CH*H*), 3.81 (s, 6H; 2OCH_3), 3.84 (s, 6H; 2OCH_3), 6.89 (m, 4H; H_{Ar}), 7.24 (d, $^3J = 6.69$ Hz, 2H; H_{Ar}), 7.29 (d, $^3J = 6.69$ Hz, 2H; H_{Ar}), 7.67 (d, $^3J = 8.04$ Hz, 2H; H_{Ar}), 7.71 (d, $^3J = 8.03$ Hz, 2H; H_{Ar}); ^{13}C NMR (75 MHz, [D$_8$]toluene, −10 °C) $\delta = -10.7$ ($ZnCH_3$), −8.5 ($ZnCH_3$), −6.6 ($ZnCH_3$), 1.0 (Si(CH_3)$_3$), 1.2 (Si(CH_3)$_3$), 19.1 ($2CH_3$), 24.5 ($2CH_3$), 24.8 (CH_2), 25.0 (CH_2), 31.8 (CH_3), 32.0 (CH_3), 35.3 (CH_2), 35.4 (CH_2), 42.5 (CH_2), 43.1 (CH_2), 46.5 (C_q), 48.0 (C_q), 50.3 (CH), 50.6 (CH), 56.3 (C_q), 56.4 (C_q), 63.9 (OCH_3), 65.3 (OCH_3), 90.7 (C_q), 91.5 (C_q), 122.5 (C_{Ar}), 122.8 (C_{Ar}), 132.8 (C_{Ar}), 133.6 (C_{Ar}), 134.1 ($C_{q,Ar}$), 134.2 ($C_{q,Ar}$), 135.1 (C_{Ar}), 135.2 (C_{Ar}), 139.3 ($C_{q,Ar}$), 139.4 ($C_{q,Ar}$), 163.9 ($C_{q,Ar}$), 164.5 ($C_{q,Ar}$); X-ray crystal data of (*R*-**3**)(*S*-**3**): $C_{42}H_{68}O_4Si_2Zn_2$, $M = 823.88$, space group $P2_1/c$, $a = 11.5901(2)$, $b = 21.9639(3)$, $c = 8.6399(1)$ Å; $\beta = 104.968(1)°$, $V = 2124.78(5)$ Å^3, $Z = 2$, $T = 200(2)$ K, $\mu = 1.223\,mm^{-1}$, reflections total: 21536, unique: 4851, observed: 4226 ($I > 2\sigma(I)$), parameters refined: 234, $R1 = 0.026$, $wR2 = 0.062$, $GOF_{all} = 1.05$.

Characterization of (*R*-4)(*S*-4): Yield: 34%, m.p. 204 °C decomposition; elemental analysis calcd (%): C 66.75, H 8.65; found: C 66.72, H 8.65; ^{1}H NMR (500 MHz, [D$_8$]toluene, +10 °C): $\delta = -0.83$ (s, 3H; $ZnCH_3$), 0.64 (s, 3H; CH_3), 1.26 (m, 2H; $2CH_2$), 1.31 (s, 6H; $2CH_3$), 1.41 (s, 9H; *t*Bu), 1.49 (m, 1H; CH_2), 1.74 (s, 1H; CH), 2.26 (m, 1H; CH_2), 2.48 (m, 1H; CH_2), 2.91 (m, 1H; CH_2), 3.81 (s, 3H; OCH_3), 6.88 (t, $^3J = 7.96$ Hz, 1H; H_{Ar}), 7.20 (dd, $^3J = 7.96$ Hz, $^4J = 1.10$ Hz, 1H; H_{Ar}), 7.58 (dd, $^3J = 8.23$ Hz, $^4J = 1.10$ Hz, 1H; H_{Ar}); ^{13}C NMR (75 MHz, [D$_8$]toluene, −10 °C) $\delta = -5.7$ ($ZnCH_3$), 18.5 (CH_3), 22.4 (CH_3), 24.4 (CH_2), 29.9 (CH_3), 32.2 (C(CH_3)$_3$), 35.2 (CH_2), 35.8 (*C*(CH_3)$_3$), 42.3 (CH_2), 42.3 (C_q), 50.1 (CH), 57.3 (C_q), 65.5 (OCH_3), 87.0 (C_q), 122.4 (C_{Ar}), 127.1 (C_{Ar}), 129.4 (C_{Ar}), 143.2 ($C_{q,Ar}$), 147.5 ($C_{q,Ar}$), 158.7 ($C_{q,Ar}$); X-ray crystal data of (*R*-**4**)(*S*-**4**): $C_{44}H_{68}O_4Zn_2$, $M = 791.72$, space group $P\bar{1}$, $a = 8.6134(2)$, $b = 10.8743(2)$, $c = 12.1678(3)$ Å; $\alpha = 66.662(1)$, $\beta = 82.935(1)$, $\gamma = 73.931(1)°$; $V = 1005.45(4)$ Å^3, $Z = 1$, $T = 200(2)$ K, $\mu = 1.233\,mm^{-1}$, reflections total: 10316, unique: 4556, observed: 4031 ($I > 2\sigma(I)$), parameters refined: 234; $R1 = 0.031$, wR2 = 0.079, $GOF_{all} = 1.06$.

Catalyses: The catalyses were performed with ligands **1**–**4** according to the following general procedure: the scalemic mixture of enantiomeric ligands in proportions from 0 to 100 (0.12 mmol as total amount of ligand, 5 mol% with respect to benzaldehyde) was treated with diethylzinc in hexane (3.3 mL, 3.0 mmol, 0.9 M) at 0 °C for 15 min. Benzaldehyde (0.24 mL, 0.25 g, 2.4 mmol) was added and this mixture was kept for 24 hours at −30 °C. After quenching with water and hydrolyzing with hydrochloric acid, the organic layer was separated, neutralized ($NaHCO_3$) and dried (Na_2SO_4). The chemical yield was analyzed by GC, and the enantiomeric excess by chiral HPLC.

Computational section: Optimizations (RHF/LanL2DZ (Zn, Si)/3-21G (C, H, O) and single point (B3LYB/LanL2DZ (Zn, Si) 6-31G* (C, H, O), X-ray geometries) computations were performed using GAUSSIAN 98.[23]

Acknowledgements

We are grateful to the Fonds der Chemischen Industrie (Sachbeihilfe and Liebig-Stipendium for B.G.), the Deutsche Forschungsgemeinschaft (GO 930/1, GO 930/2, GO 930/3, GO 930/4), the Research Pool Foundation of the University of Heidelberg for financial support and the Degussa AG and the BASF AG for generous gifts of chemicals. We thank Prof. Dr. P. Hofmann for generous support at Heidelberg.

[1] a) L. Pu, H.-B. Yu, *Chem. Rev.* **2001**, *101*, 757–824; b) *Comprehensive Asymmetric Catalysis*, *Vol. I–III* (Eds.: E. N. Jacobsen, A. Pfaltz, H. Yamamoto), Springer, Heidelberg, **1999**.

[2] a) S. C. Stinson, *Chem. Ing. News* **2000**, May 8, 59–70; b) L. Tan, C. Chen, R. D. Tillyer, E. J. J. Grabowski, P. J. Reider, *Angew. Chem.* **1999**, *111*, 724–726; *Angew. Chem. Int. Ed.* **1999**, *38*, 711–713.

[3] N. K. Anand, E. M. Carreira, *J. Am. Chem. Soc.* **2001**, *123*, 9687–9688.

[4] M. Kitamura, S. Okada, S. Suga, R. Noyori, *J. Am. Chem. Soc.* **1989**, *111*, 4028–4036.

[5] a) M. Yamakawa, R. Noyori, *Organometallics* **1999**, *18*, 128–133; b) M. Yamakawa, R. Noyori, *J. Am. Chem. Soc.* **1995**, *117*, 6327–6335.

[6] a) B. Goldfuss, M. Steigelmann, S. I. Khan, K. N. Houk, *J. Org. Chem.* **2000**, *65*, 77–82; b) B. Goldfuss, M. Steigelmann, F. Rominger, *Eur. J. Org. Chem.* **2000**, 1785–1792.

  0947-6539/02/0822-5217 $ 20.00+.50/0

[7] The term "scalemic" describes an unequal mixture of enantiomers: C. H. Heathcock, B. L. Finkelstein, E. T. Jarvi, P. A. Radel, C. R. Hadley, *J. Org. Chem.* **1988**, *53*, 1922 – 1942.
[8] C. Puchot, O. Samuel, E. Dunach, S. Zhao, C. Agami, H. B. Kagan, *J. Am. Chem. Soc.* **1986**, *108*, 2353 – 2357.
[9] M. Kitamura, S. Suga, K. Kawai, R. Noyori, *J. Am. Chem. Soc.* **1986**, *108*, 6071 – 6072.
[10] a) P. I. Dosa, C. Fu, *J. Am. Chem. Soc.* **1998**, *120*, 445 – 446; b) E. Rijnberg, N. J. Hovestad, A. W. Kleij, J. T. B. H. Jastrzebski, J. Boersma, M. D. Janssen, A. L. Spek, G. van Koten, *Organometallics* **1997**, *16*, 2847 – 2857; c) T. Wirth, K. J. Kulicke, G. Fragale, *Helv. Chim. Acta* **1996**, *79*, 1957 – 1966; d) K. Fitzpatrick, R. Hulst, R. M. Kellogg, *Tetrahedron: Asymmetry* **1995**, *6*, 1861 – 1864; e) C. Bolm, G. Schlingloff, K. Harms, *Chem. Ber.* **1992**, *125*, 1191 – 1203.
[11] C. Girard, H. B. Kagan, *Angew. Chem.* **1998**, *110*, 3088 – 3127; *Angew. Chem. Int. Ed.* **1998**, *37*, 2923 – 2959.
[12] a) M. Kitamura, H. Oka, R. Noyori, *Tetrahedron* **1999**, *55*, 3605 – 3614; b) M. Kitamura, S. Suga, H. Oka, R. Noyori, *J. Am. Chem. Soc.* **1998**, *120*, 9800 – 9809.
[13] N. Oguni, Y. Matsuda, T. Kaneko, *J. Am. Chem. Soc.* **1988**, *110*, 7877 – 7878.
[14] a) D. G. Blackmond, *J. Am. Chem. Soc.* **2001**, *123*, 545 – 553; b) H. B. Kagan, *J. Am. Chem. Soc.* **1999**, *121*, 9299 – 9306.
[15] B. Goldfuss, M. Steigelmann, F. Rominger, H. Urtel, *Chem. Eur. J.* **2001**, *7*, 4456 – 4464.
[16] The enantiomeric purity of the anisyl fenchols is expected to correlate with the enantiomeric purity of the commercially available (−)-/(+)-fenchone.
[17] a) B. Goldfuss, M. Steigelmann, *J. Mol. Mod.* **2000**, *6*, 166 – 170; b) B. Goldfuss, S. I. Khan, K. N. Houk, *Organometallics* **1999**, *18*, 2927 – 2929.
[18] B. Goldfuss, M. Steigelmann, F. Rominger, *Angew. Chem.* **2000**, *112*, 4299 – 4302; *Angew. Chem. Int. Ed.* **2000**, *39*, 4133 – 4136.
[19] The marking (*R*) refers to the second stereogenic center of the bicycloheptane moiety and elucidates that the ligand system is based on (−)-fenchone.
[20] Analogous structures can be expected in toluene or in hexanes, due to similar polarities of the solvents.
[21] The racemic ligand mixture yields crystals containing both enantiopure dimeric complexes side by side in the unit cell.
[22] a) P. J. Hay, W. R. Wadt, *J. Chem. Phys.* **1985**, *82*, 270; b) W. R. Wadt, P. J. Hay, *J. Chem. Phys.* **1985**, *82*, 284; P. J. Hay, W. R. Wadt, *J. Chem. Phys.* **1985**, *82*, 299.
[23] Gaussian 98, Revision A.7; M. J. Frisch, G. W. Trucks, H. B. Schlegel, G. E. Scuseria, M. A. Robb, J. R. Cheeseman, V. G. Zakrzewski, J. A. Montgomery Jr., R. E. Stratmann, J. C. Burant, S. Dapprich, J. M. Millam, A. D. Daniels, K. N. Kudin, M. C. Strain, O. Farkas, J. Tomasi, V. Barone, M. Cossi, R. Cammi, B. Mennucci, C. Pomelli, C. Adamo, S. Clifford, J. Ochterski, G. A. Petersson, P. Y. Ayala, Q. Cui, K. Morokuma, D. K. Malick, A. D. Rabuck, K. Raghavachari, J. B. Foresman, J. Cioslowski, J. V. Ortiz, A. G. Baboul, B. B. Stefanov, G. Liu, A. Liashenko, P. Piskorz, I. Komaromi, R. Gomperts, R. L. Martin, D. J. Fox, T. Keith, M. A. Al-Laham, C. Y. Peng, A. Nanayakkara, C. Gonzalez, M. Challacombe, P. M. W. Gill, B. Johnson, W. Chen, M. W. Wong, J. L. Andres, M. Head-Gordon, E. S. Replogle, J. A. Pople, Gaussian, Inc., Pittsburgh PA, **1998**.
[24] The *t*Bu group is smaller than $SiMe_3$ ($C-C_{Me}$ 1.53 Å; $Si-C_{Me}$: 1.86 Å), but is closer to the benzene ring due to the shorter C–C bond ($C_{ar.}-C$: 1.55 Å compared with the C–Si distance ($C_{ar.}-Si$: 1.90 Å).

Received: May 14, 2002 [F4092]

  0947-6539/02/0822-5218 $ 20.00+.50/0